

## Effect of adsorption of $^3\text{He}$ and $^4\text{He}$ on the low-temperature ultrasonic properties of porous Vycor

Norbert Mulders\*

*Department of Physics and Astronomy, University of Delaware, Newark, Delaware 19716*

Eric Molz and John R. Beamish

*Department of Physics, University of Alberta, Edmonton, Alberta, Canada T6G 2J1*

(Received 4 January 1993)

Ultrasonic measurements show that porous Vycor glass has a two-level system (TLS) density of states and a one-phonon-TLS coupling strength very similar to  $\alpha\text{-SiO}_2$ . In addition, because of the sharply reduced sound speed in Vycor, the effect of the first-order Raman process is clearly observable. Introduction of  $^3\text{He}$  and  $^4\text{He}$  in the pore space causes an increase of the TLS relaxation rates. This results in a shift to lower temperature of the relaxation contribution to the changes in the sound speed and the ultrasonic attenuation. The effect is strongly coverage dependent. This can be most clearly observed in the ultrasonic attenuation around 100 mK. With  $^3\text{He}$  we observe a gradual increase with coverage  $n$ , which saturates for  $n > 22 \mu\text{mol}/\text{m}^2$ . With  $^4\text{He}$  we see similar behavior for low  $n$ , but the attenuation reaches a maximum for  $n$  close to  $n_c$ , the critical coverage for the onset of superfluidity. For higher coverage it drops back to approximately half its maximum value. With completely filled pores the contribution to the sound speed shows a clear scaling with  $T^4/\omega$ , in contrast to the  $T^3/\omega$  or  $T^7/\omega$  behavior expected for the direct and Raman relaxation processes.

### INTRODUCTION

Amorphous materials have low-temperature properties that differ considerably from those of their crystalline counterparts.<sup>1</sup> Characteristic are, among others, a linear temperature dependence of the specific heat, a variation in the sound speed proportional to  $\ln(T)$ , and a saturable component to the acoustic attenuation. Most of this anomalous behavior is rather successfully explained by the tunneling model, originally introduced by Phillips<sup>2</sup> and Anderson, Halperin, and Varma.<sup>3</sup> This model draws attention to the role of the numerous structural defects in glasses. It is assumed that these give rise to localized two-level tunneling states with a nearly constant density of states over a very wide range of energies. Furthermore, these two-level systems (TLS) couple strongly to elastic strain fields, which results in a range of resonant and relaxation phenomena.

In the interior of dielectric glasses the normal channel for relaxation of the TLS population is provided by an interaction with the thermal phonons. Near a surface, TLS may also interact with excitations in any material adsorbed on that surface. In an interesting experiment Schubert, Leiderer, and Kinder<sup>4</sup> showed that the transmission of 25-GHz longitudinal phonons from crystalline quartz into an amorphous paraffin film is greatly enhanced by the adsorption of a 10-Å helium film onto the paraffin. They attributed this to an increased critical intensity for the resonant interaction between the phonons and TLS in the paraffin. This occurs because interaction with the helium strongly increases the TLS relaxation rates. Beamish, Hikata, and Elbaum,<sup>5</sup> in an ultrasonic experiment at much lower frequencies, and Chan *et al.*<sup>6</sup> in measurements of the dielectric constant, reached a similar conclusion for the relaxation rates in a

porous silica glass. When helium was admitted into the pore space the relaxation contribution to the change in sound speed increased substantially.

The strong coupling between excitations in the helium and the TLS in the glass opens the possibility of studying the properties of thin helium films through their effects on the relaxation rates of the TLS in the substrate. One might expect that changes in the excitation spectrum associated with layer completion or a superfluid transition would be observable in the low-temperature properties of the substrate. In many cases, however, these effects are masked by the much larger contributions of the adsorbate alone. Measurements of the specific heat, for example, are completely dominated by the contribution of the helium film. In measurements of the dielectric constant or the shear modulus, where the direct helium contribution is small or zero, TLS-helium effects should be more readily observable. To maximize the interaction with the helium film, most of the TLS should be close to a surface. This restricts the possible substrates to thin films, fine powders, or microporous solids. In this paper we report the results of an investigation of the effects of helium on the TLS relaxation rates in porous Vycor glass (Corning 7930), as seen in its acoustic properties. For ultrasonic experiments Vycor is an excellent substrate. It displays all the low-temperature characteristics of amorphous silica and essentially all of the solid is within 100 Å of the pore walls. Acoustic losses are sufficiently small to make measurements on practical size samples.

### EXPERIMENT

We have made ultrasonic measurements of the temperature dependence of the transverse sound speed and attenuation in porous Vycor glass. The Vycor sample was

mounted in a copper cell attached to the mixing chamber of a small dilution refrigerator. Helium could be admitted to the cell from a room-temperature gas handling system consisting of a calibrated volume and a capacitive pressure sensor. Starting with empty samples, known amounts of either  $^3\text{He}$  or  $^4\text{He}$  were added. Thus we obtained sets of data for fixed helium coverage. To obtain a uniform film thickness it is important that the films are properly annealed. The helium has to be admitted at a temperature where the pressure is sufficiently high to provide adequate mass transport through the vapor. This may require temperatures as high as 10 K for the thinnest  $^4\text{He}$  films. The temperature is then gradually lowered, usually by the simple expedient method of initially taking the data on cooling. To check for equilibrium at least some data were taken both on cooling and warming.

The cell temperature was measured with a calibrated Ge thermometer and could be controlled to within 1 mK. The temperature range over which data could be taken was strongly dependent on coverage. With increasing film thickness desorption occurs at lower temperatures, especially with  $^3\text{He}$ , so that higher temperature data could only be taken for thin films or when the pores were completely filled. With  $^4\text{He}$  above a critical film thickness, a superfluid transition takes place at some temperature. The decoupling of a part of the superfluid fraction then causes changes in the sound speed which for thicker films are larger than the changes due to TLS effects.

Porous Vycor glass is made from a boron-rich glass-forming melt which on cooling undergoes spinodal decomposition into boron-rich and silica-rich phases. The former is leached out, leaving a completely interconnected pore structure in a high silica glass matrix. Small-angle neutron scattering<sup>7</sup> and transmission electron microscope experiments<sup>8</sup> reveal a characteristic length scale of 200 Å. For our samples we measured a density  $\rho = 1.48 \text{ g/cm}^3$ , a porosity  $\phi = 0.28$ , and a specific surface area  $S = 105 \text{ m}^2/\text{g}$ . This gives an effective cylindrical pore radius of 35 Å. The samples, cylindrical rods with a diameter of 3 mm and approximately 10 mm long, were cleaned in hydrogen peroxide at 80°C, followed by rinsing in distilled water and drying in air. Although the samples were subsequently evacuated to remove most of the remaining water, installation in the experimental cell involved exposure to air and, although the cell was reevacuated, the samples must contain some adsorbed gases and water.

The ultrasonic sound speed and attenuation measurements were performed using a pulse echo method.<sup>9</sup> The resolution in changes in the sound speed was  $\Delta v/v_0 = 1 \text{ ppm}$  and for the attenuation  $\Delta\alpha = 0.005 \text{ dB}$ . We used 20-MHz  $\text{LiNiO}_3$  shear mode transducers bonded to opposite ends of the sample with high viscosity silicone oil. It was possible to do experiments over a continuous range of frequencies between 4 and 30 MHz and up to 180 MHz at the odd harmonics of the transducers. Computer control of the ultrasonic system made it possible to take measurements over a range of frequencies virtually simultaneously. To make comparison between data sets for different film thicknesses possible, long-term drift in the

ultrasonic system, mostly associated with variations in the ambient temperature, had to be eliminated. This was accomplished by taking reference measurements at each temperature setpoint, thus maintaining a long-term stability of the same order as the resolution of the system.

### THE STANDARD MODEL

The consequences of the standard tunneling model for the low-temperature acoustic properties of glass were developed by various authors during the 1970s, culminating in a paper by Doussineau *et al.*<sup>10</sup> which summarizes the standard results and extends these to higher-order relaxation processes and a more general TLS distribution function. We will follow their conventions. In the tunneling model the TLS is treated as a particle in an asymmetric double-well potential. The energies of the two lowest eigenstates, the only ones considered in the theory, are  $E_{\pm} = \pm(\Delta^2 + \Delta_0^2)^{1/2}$ , where  $2\Delta$  is the potential asymmetry and  $\Delta_0$  the tunneling amplitude. This picture of the nature of the TLS does not offer much guidance for the construction of a density of states. In the standard tunneling model one uses a distribution function originally introduced by Phillips<sup>2</sup> of the form [in terms of  $E$  and  $r = (\Delta_0/E)^2$ ]

$$P(E, r) \propto (1-r)^{-1/2} r^{-1}. \quad (1)$$

This form is too restrictive to accommodate all experimental results. To alleviate this problem, Doussineau *et al.*<sup>10</sup> proposed a modification

$$P(E, r) \propto (1-r)^{\mu-1/2} r^{-1}. \quad (2)$$

Its main virtue, beyond keeping the further mathematics tractable, is that with an appropriate choice of  $\mu$  it is possible to describe both the low- and the high-temperature behavior of the change in sound speed, while maintaining a plateau in the ultrasonic attenuation. To make  $P(E, r)$  normalizable one has to assume cutoffs on  $r$  and  $E$ . In the frequency and temperature ranges over which we have performed our experiments their actual values play no role.

The TLS interact with a sound wave through two distinct mechanisms. At very low temperatures only the resonant interaction between the sound wave and TLS with appropriate level splitting is important. It causes an increase in the sound speed,

$$\frac{\Delta v}{v_0} = \frac{C}{1+2\mu} \ln(T/T_0) \quad (3)$$

with  $T_0$  some arbitrary reference temperature, and

$$C = \rho \gamma^2 / \rho v_0, \quad (4)$$

where  $\rho$  is the average density of states,  $\gamma$  the coupling constant for the one-phonon-TLS interaction,  $\rho$  the solid density, and  $v_0$  the sound speed. In our experiments the resonant attenuation is completely saturated and hence unobservable.

At higher temperatures a second mechanism becomes important. Modulation of the TLS energy splitting by the passing sound wave drives the TLS population out of

equilibrium. Relaxation towards equilibrium takes place via an interaction with the thermal phonons. The relaxation time depends on the TLS parameters  $E$  and  $r$  as well as the temperature,  $T$ . At low temperatures only the one-phonon or direct process is of importance, but with increasing temperature the two-phonon, Raman process starts to dominate the relaxation rates. The relaxation processes cause a change in elastic constant,  $c$ , given by

$$\frac{\Delta c}{c_0} = \int d(\beta E) \operatorname{sech}^2 \beta E \int dr \frac{(1-r)^{\mu+1/2}}{r(1+i\omega\tau)}. \quad (5)$$

The relaxation time  $\tau$  is the result of two parallel processes,  $\tau^{-1} = (\tau_R)^{-1} + (\tau_D)^{-1}$ , with the relaxation time for the direct process given by

$$\tau_D = rK_3 T^3 F_3(\beta E) \quad (6)$$

with

$$K_3 = \frac{4k_B^3}{\pi^3 \hbar^4} \sum_{\sigma} \frac{\gamma_{\sigma}^2}{\rho v_{\sigma}^5},$$

$$F_3(u) = u^3 \coth(u),$$

and the relaxation time for the Raman process

$$\tau_R = rK_7 T^7 F_7(\beta E) \quad (7)$$

with

$$K_7 = \frac{k_B^7}{\pi^3 \hbar^7} \sum_{\sigma, \tau} \frac{\delta_{\sigma\tau}^2}{(\rho v_{\sigma}^5)(\rho v_{\tau}^5)},$$

$$F_7(u) = \frac{u}{70} (u^2 + \pi^2) \left[ u^4 - \pi^2 u^2 + \frac{10}{3} \pi^4 \right] \coth(u).$$

The summations are over the phonon polarizations, and  $\delta$  is the coupling constant for the Raman process. The change in sound speed and attenuation are obtained from the real and imaginary parts of  $c$  by

$$\frac{\Delta v}{v_0} = \frac{1}{2} \operatorname{Re} \frac{\Delta c}{c_0}, \quad (8)$$

$$\alpha = \frac{\omega}{v_0} \operatorname{Im} \frac{\Delta c}{c_0}. \quad (9)$$

Although the tunneling model has been successful in explaining many of the experimental observations on amorphous systems, it is of a rather *ad hoc* nature, reflecting our poor understanding of these systems on a microscopic level. In recent years many attempts have been made to explain the remarkably similar properties of different glasses.<sup>11</sup> Much effort has been concentrated on incorporating the TLS-TLS interaction mediated by the phonons, to which the TLS are supposed to couple so strongly. Polaron theory type calculations by Kassner and Silbey,<sup>12</sup> for example, seem to indicate that this leads to a renormalization of the TLS parameters, and much smaller relaxation rates for the TLS than one would expect on the basis of the standard model. Unfortunately, these theories have not yet been developed far enough to make direct contact with the experiments. We will therefore discuss further results within the framework of the

standard model, bearing in mind that numerical results are more of the nature of fitting parameters to a semi-empirical model than reflecting true insight into such quantities as the density of states or the TLS-phonon interaction strength.

### EMPTY VYCOR

The microporous structure of Vycor does not seem to cause essential changes in the glassy behavior of the silica. Figure 1 shows the variation with temperature of the transverse sound velocity for a range of frequencies. The change in sound speed is given by the sum of the resonant and relaxation contributions. At low temperatures, where the relaxation contribution is negligible, we see a (frequency-independent) change in sound speed  $\Delta v/v_0 = C' \ln(T/T_0)$ , with  $C' = C/(1+2\mu)$ , while at high temperatures, with the Raman process dominant, we get  $\Delta v/v_0 = -(1/2)C \ln(T^7/\omega) +$  the resonant contribution. The low- and high-temperature data can be used to determine  $C$ ,  $\mu$ , and  $K_7$ . In our experiments the temperature range over which the direct relaxation process is dominant is usually too small to make it possible to obtain  $K_3$  from a direct fit. However, as can be seen from Fig. 2, the observed temperature of the maximum in the velocity,  $T_{\max}$ , is proportional to  $f^{1/3}$  (with  $f$  the ultrasonic frequency). This is exactly what one would expect if in the vicinity of the velocity maximum the direct process were dominant. Numerical evaluation of Eq. (5) with only the direct relaxation process included gives  $\ln(K_3 T_{\max}^3/\omega) = 1.6$  (using  $\mu = 0.25$ ). We use this relation together with the data shown in Fig. 2 to obtain  $K_3$ . From  $C_l$ ,  $C_t$ , and  $K_3$ , using Eqs. (4) and (6), one can then find  $\rho$ ,  $\gamma_l$ , and  $\gamma_t$ . The subscripts  $l$  and  $t$  refer to the longitudinal and transverse sound modes.  $C_l$  was obtained from measurements of the longitudinal sound speed which we do not further discuss here. The results are given in Table I which also contains the values for  $a$ -SiO<sub>2</sub>.<sup>13</sup> We find essentially the same values for  $\gamma_l$  and  $\gamma_t$  in Vycor as in  $a$ -SiO<sub>2</sub>. The densities of state are also of the same magnitude. The rather close agreement be-

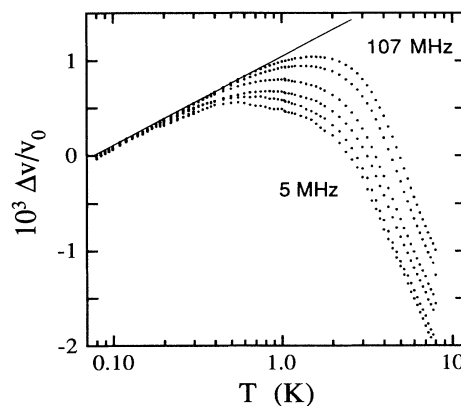


FIG. 1. The change in sound speed in empty Vycor for 5, 8, 15, 24, 64, and 107 MHz. The straight line indicates the resonant contribution.

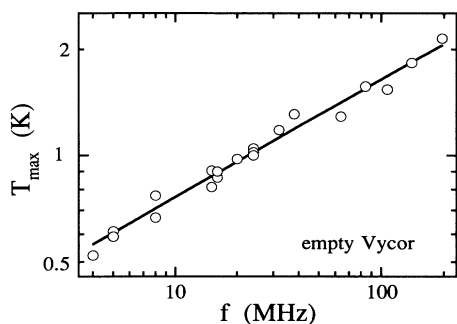


FIG. 2. The temperature of the maximum in the sound speed in empty Vycor vs the ultrasonic frequency. The line is a fit to  $T_{\max} = af^{1/3}$ .

tween the coupling constants may well be fortuitous. The value of  $K_3$  is determined from  $T_{\max}(\omega)$  and is rather strongly dependent on  $\mu$ . A change in  $\mu$  from 0.25 to zero increases the estimate of  $K_3$  by a factor of 4 and leads to coupling constants which are about twice as high as given in Table I.

It can be seen from the preceding equations that if one of the relaxation processes is dominant, the relaxation contribution to the acoustic properties becomes a function of a unique combination of  $T$  and  $\omega$ . In the case of the direct process this is  $T^3/\omega$ , while with the Raman process dominant, the scaling variable is  $T^7/\omega$ . The relaxation contributions are easily separated out by determining the resonant contribution at low temperatures and subtracting it off over the whole temperature range. The region over which the Raman process dominates is quite well defined. This is best seen from Fig. 3 which shows the same data as Fig. 1 but with the resonant contribution subtracted and plotted against  $T^7/\omega$ . In the same figure we also show data for a second, similar sample. Quite clearly the Raman contribution is strongly sample dependent.

The Raman contribution becomes prominent at rather lower temperatures than is usually the case in solid  $a$ - $\text{SiO}_2$ . We attribute this to the strong dependence of  $K_7$  on the sound speeds,  $K_7 \sim 1/v^{10}$ . The sound speeds in Vycor are barely 60% of those in solid  $a$ - $\text{SiO}_2$ . Consequently one would expect that the temperature scale for

TABLE I. The parameters in the tunneling model for Vycor and  $a$ - $\text{SiO}_2$ .

	Vycor	$a$ - $\text{SiO}_2$
$\rho$ (g/cm <sup>3</sup> )	1.48	2.20
$v_1$ (km/s)	3.45	5.80
$v_t$ (km/s)	2.19	3.80
$C_1(10^{-4})$	5.8	3.1
$C_t(10^{-4})$	6.5	2.9
$K_3(10^8\text{K}^{-3}\text{s}^{-1})$	7.8	4.0
$K_7(10^5\text{K}^{-7}\text{s}^{-1})$	1.5	
$\gamma_1$ (eV)	1.08	1.04
$\gamma_t$ (eV)	0.74	0.65
$\mathcal{A}(10^{45}\text{J}^{-1}\text{m}^{-3})$	0.49	0.80

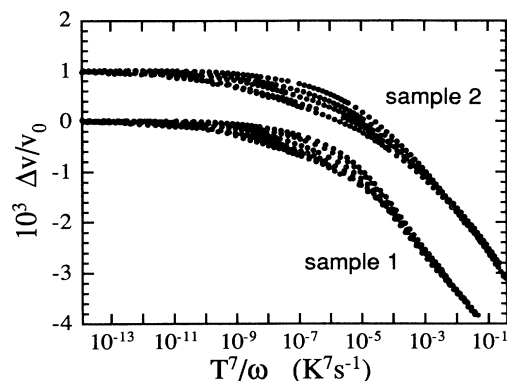


FIG. 3. The relaxation contribution to the sound speed in empty Vycor. Sample 1 was mounted under a  $^4\text{He}$  atmosphere, sample 2 was exposed to air. The data shown are the for following frequencies: Sample 1: 5, 8, 15, 24, 64, and 107 MHz; sample 2: 5, 8, 16, 32, and 98 MHz.

the Raman process in Vycor is compressed by a factor of 0.45. In empty Vycor the TLS interact with phonons supported by the glass skeleton. In a porous substrate one must distinguish between phonons with wavelengths that exceed the size of the structural units, here some 200 Å, and those that have shorter wavelengths. The propagation speed of the first class is the ultrasonic sound speed, the latter have the higher sound speed characteristic of the bulk solid. In Vycor the crossover takes place for phonons with an energy around 5–10 K. One may expect, in view of the strong dependence of the relaxation rates on the sound speed, to see this crossover in the temperature dependence of the ultrasonic properties. It is often stated that thermal phonons with an energy of a few times  $k_B T$  have the strongest effect and there should be a crossover to a weaker temperature dependence of the sound speed around 2–4 K. We do not observe this. However, the Raman process, which is often not considered, gives more weight to the low-energy phonons and the crossover takes place at much higher temperatures. Numerical calculations which include the change in sound speed support this view.

We can now use the TLS parameters obtained from the velocity data to calculate the ultrasonic attenuation. Figure 4(a) shows a comparison between calculated and measured values of the attenuation. Because, according to Eq. (9),  $\alpha = l^{-1} \propto \omega$ , it is most convenient to plot the attenuation per wavelength,  $l^{-1}\lambda$ . We see that at intermediate temperature the calculations systematically underestimate the actual values of the attenuation. On the other hand, the calculations predict the right plateau height, which strongly supports our choice to determine  $C$  from the Raman slope instead of using the resonant contribution. Figure 4(b) shows a similar comparison for the sound speed.

#### THIN FILMS

When helium is adsorbed in the pore space, the sound speed and attenuation in Vycor change significantly. Fig-

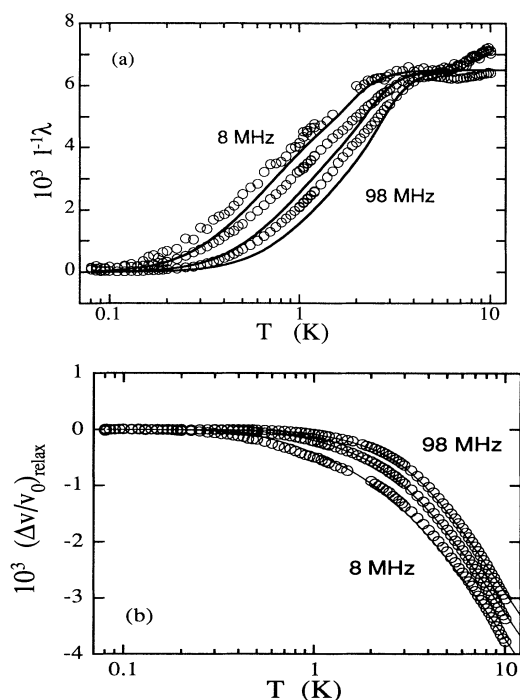


FIG. 4. (a) The change in ultrasonic attenuation in empty Vycor, for 8, 32, and 98 MHz. The curves are calculated using Eqs. (5)–(9) and the parameters in Table I. (b) A comparison between the calculated and measured relaxation contribution to the sound speed in empty Vycor, for 8, 32, and 98 MHz. The curves are calculated using Eqs. (5)–(9) and the same parameters as in (a).

Figure 5 shows the sound speed as a function of temperature for a range of  $^3\text{He}$  coverages, from empty Vycor up to a coverage of  $32 \mu\text{mol}/\text{m}^2$ . Increasing the amount of helium in the pores causes a decrease in the sound velocity due to the added mass of the helium and at low temperatures the shift in sound speed is proportional to the

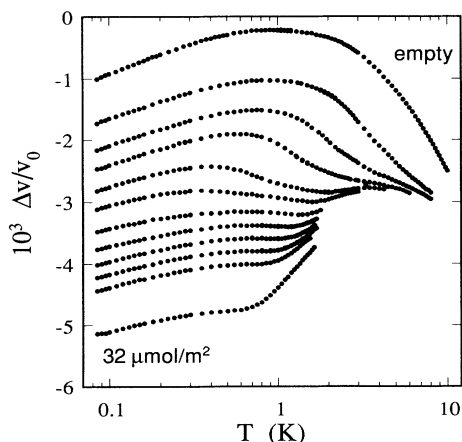


FIG. 5. The change in sound speed, at 16 MHz, for empty Vycor and  $^3\text{He}$  films with coverages of 7.8, 12.1, 15.0, 17.6, 19.3, 20.9, 22.3, 23.8, 25.3, 26.8, and  $31.8 \mu\text{mol}/\text{m}^2$ .

change in the total density. The resonant slopes are essentially independent of coverage. This indicates that the product of the TLS density of states and the TLS-phonon coupling constant ( $\lambda\gamma^2$ ) is not affected by the adsorption of helium. When the temperature is increased, the helium starts to desorb. This results in a drop in the effective density of the sample and consequently in an increase of the sound speed. At a coverage of  $12.1 \mu\text{mol}/\text{m}^2$  this becomes noticeable as positive curvature in the sound speed around 4 K. With increasing film thickness the atoms become more weakly bound to the surface and desorption begins at lower temperatures, as illustrated by the steep rise in the sound speed starting already around 0.9 K when  $32 \mu\text{mol}/\text{m}^2$  is absorbed.

That the helium has an effect on the TLS relaxation rates can be seen from the shift in  $T_{\text{max}}$ . This is most noticeable in the first few films. For higher coverage it becomes difficult to judge the position of the velocity maximum due to the strong effect that the desorption has on the sound speed. However, with full pores we find  $T_{\text{max}} = 400 \text{ mK}$ , comparable to what we already see in a relatively thin film. It seems that the relaxation rates increase rapidly with film thickness up to a coverage of about  $20 \mu\text{mol}/\text{m}^2$  after which they remain roughly constant. We see similar behavior in the attenuation measurements. Figure 6 shows the attenuation, again as a function of temperature for increasing film thickness. At low temperature there is a gradual increase in the attenuation with film thickness. This effect saturates again at a coverage of about  $20 \mu\text{mol}/\text{m}^2$ . Further increasing the film thickness has no effect on the acoustic properties anymore. At higher temperatures we also observe a broad bump in the attenuation, especially pronounced in the  $7.8 \mu\text{mol}/\text{m}^2$  data at a temperature around 2 K, which is not a feature of the standard tunneling model. Its size and shape are strongly dependent on coverage. It is also rather sensitive to the sample preparation. Surprisingly, samples which we believe to be least contaminated with air show the most pronounced effect. We do not know if it is intrinsic to porous glass.

We also studied the effect of  $^4\text{He}$  on the relaxation

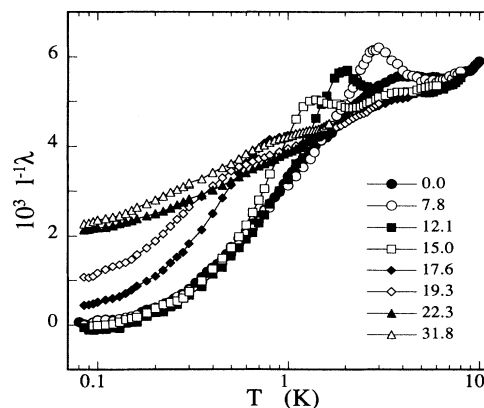


FIG. 6. The attenuation, at 16 MHz, for  $^3\text{He}$  films, starting with empty Vycor up to a coverage of  $32 \mu\text{mol}/\text{m}^2$ . The numbers in the figure give the coverage in  $\mu\text{mol}/\text{m}^2$ .

rates. Liquid- $^4\text{He}$  films will become superfluid below some thickness-dependent transition temperature  $T_c$ . However, on most substrates the first few monolayers form a dense, solidlike layer that remains normal at any temperature.<sup>14</sup> A critical coverage,  $n_c$ , is required before a superfluid transition takes place. Thicker films become superfluid below a transition temperature which for  $30 \mu\text{mol}/\text{m}^2 < n < 40 \mu\text{mol}/\text{m}^2$  is linear in  $n$ ,  $T_c \sim n - n_c$ .<sup>15</sup> In Vycor  $n_c = 28 \mu\text{mol}/\text{m}^2$ . Uncertainties in the surface area of the sample and sometimes also in the initial amount of helium in the sample make it difficult to prepare a film of exactly the critical coverage. We filled the sample in steps of about 1 mmol and used the measured  $T_c$  of the superfluid films, together with the linear relation between  $T_c$  and the coverage to determine the amount of helium which in our sample corresponds to  $n_c$ . We then found that one of our films corresponded to  $n = n_c \pm 150 \text{ nmol}/\text{m}^2$  or  $T_c = 0 \pm 15 \text{ mK}$ .

Figure 7 shows again the sound speed as a function of temperature and coverage. The changes in sound speed are similar to what one observes with  $^3\text{He}$ , although the desorption takes place at a somewhat higher temperature. The decoupling of the superfluid fraction from the shear motion of the sound wave causes the velocity to rise steeply at the transition (indicated by arrows in Fig. 7). We observe again a downward shift in  $T_{\text{max}}$  with increasing coverage. It reaches a minimum for  $n = 25 \mu\text{mol}/\text{m}^2$ , increases slightly when  $n$  approaches the critical coverage, after which it falls rapidly to some limiting value at about  $30 \mu\text{mol}/\text{m}^2$ . Filling the sample further, in this case up to 25 bars, does not have any influence on the sound speed beyond what one would expect to see from the added mass.

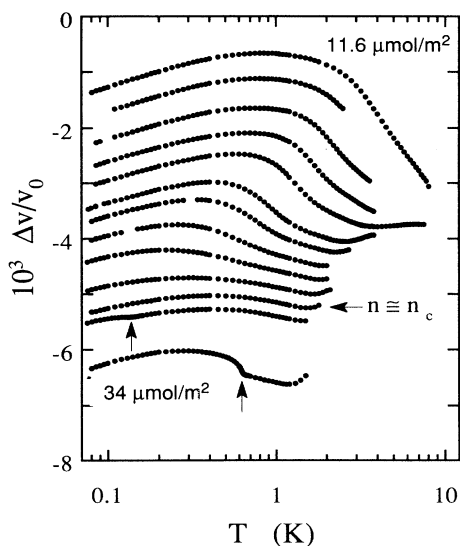


FIG. 7. The change in sound speed at 15 MHz, for Vycor with  $^4\text{He}$  film coverages of 11.6, 14.2, 16.7, 18.7, 20.6, 22.5, 23.5, 24.7, 25.8, 27.0, 28.1, 29.2, and  $34 \mu\text{mol}/\text{m}^2$ . The vertical arrows indicate the superfluid transition in the two thickest films. The third film from the bottom corresponds to a coverage close to  $n_c$ .

While the sound velocity data are roughly comparable to the  $^3\text{He}$  results, the attenuation data shows more structure. Figure 8(a) shows the attenuation results for films up to the critical coverage. The results for thicker films, up to full pores, are shown in Fig. 8(b). The little peaks (again indicated by arrows) are associated with critical attenuation at the superfluid transition. The thinner film data are rather similar to the  $^3\text{He}$  results, but instead of a saturation for higher coverages, we see that the attenuation at low temperatures drops again. The maximum attenuation is reached very close to  $n_c$ . This is shown in more detail in Fig. 9. It shows data for films at and close to the critical coverage. The difference in the effects of  $^3\text{He}$  and  $^4\text{He}$  on the attenuation are most readily observed at low temperatures. In Fig. 10 we have plotted the attenuation at a fixed temperature of 100 mK as a function of coverage. With  $^4\text{He}$  the attenuation peaks sharply close to the critical coverage to fall back to about half its peak value at higher coverage. With  $^3\text{He}$  it rises to a plateau with a height comparable to the height of the peak in the  $^4\text{He}$  case. The fact that with  $^3\text{He}$  the attenuation starts to rise at lower coverage than with  $^4\text{He}$  probably reflects the considerable difference in density of the two isotopes. It appears that, at least at coverages below  $28 \mu\text{mol}/\text{m}^2$ , films with comparable thickness in monolayers have a similar effect on the low-temperature attenuation.

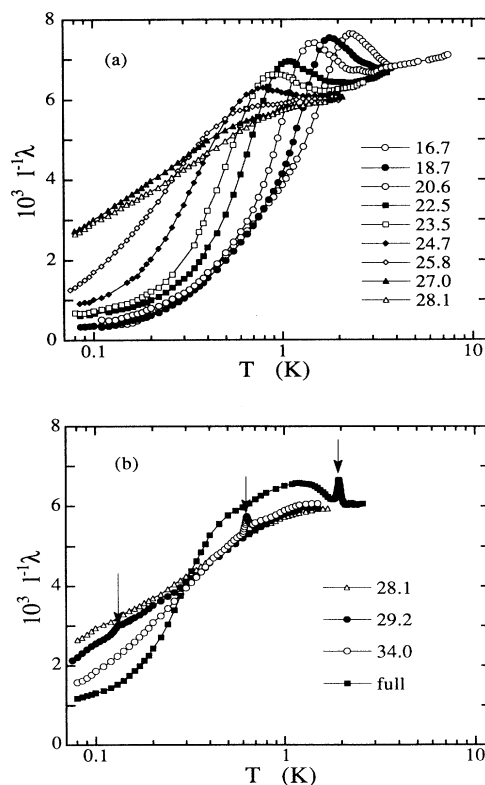


FIG. 8. (a) The attenuation at 15 MHz, for nonsuperfluid  $^4\text{He}$  films. (Coverage given in  $\mu\text{mol}/\text{m}^2$ .) (b) The attenuation at 15 MHz, for films with  $n \geq n_c$ . The arrows indicate the superfluid transition.

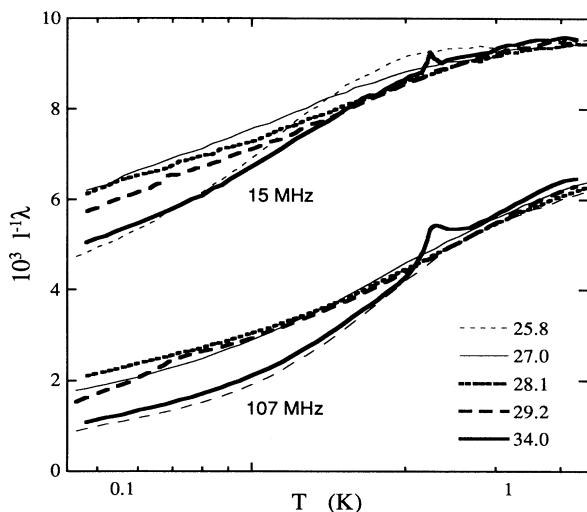


FIG. 9. The attenuation at 15 and 107 MHz for  $^4\text{He}$  films close to the critical coverage. (Coverage given in  $\mu\text{mol}/\text{m}^2$ .)

#### THICK FILMS AND FULL PORES

When the sample is filled to about 50%, further adsorption of helium does not have much effect on the acoustic properties of the system. Below 0.5 K one cannot distinguish between the effects of films with a coverage greater than approximately  $35 \mu\text{mol}/\text{m}^2$  and full pores. For  $T > 1$  K the comparison is complicated by desorption, as illustrated by Fig. 11. With  $^4\text{He}$  the superfluid transition also gives rise to a critical attenuation peak and below the transition there is some decoupling of the superfluid from the shear motion of the sample. However, we believe that the case of full pores at saturated vapor pressure is representative for a wide range of coverages. In the remainder of this section we will concentrate on the full pores case.

The main results are shown in Figs. 12–14. Measure-

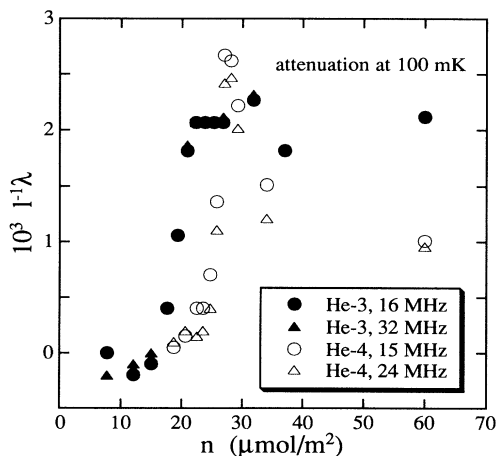


FIG. 10. The attenuation in Vycor at 100 mK as a function of film thickness.

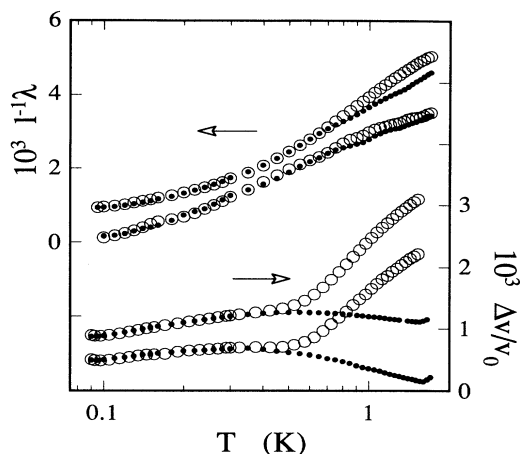


FIG. 11. A comparison between a  $38.4 \mu\text{mol}/\text{m}^2$   $^3\text{He}$  film (open symbols) and full pores (closed symbols) for the sound speed and attenuation at 8 MHz (lower curves) and 99 MHz (upper curves).

ments show again an increase of the sound speed at low temperatures (Fig. 12) which we attribute to the resonant process. The slope of the resonant contribution remains unchanged from its value for empty Vycor. Apparently we are still sampling the same TLS distribution. At higher temperatures the relaxation process causes a decrease in sound speed. Compared with empty Vycor the maximum in the sound speed is shifted to much lower temperatures, indicating a strong increase in the TLS relaxation rates due to the presence of the helium in the pore space. To further investigate this, we subtract the resonant part, in the same way as before for the empty sample. For empty Vycor at these temperatures one would then expect the data to collapse onto a single curve when plotted against  $T^3/\omega$ , the appropriate scaling variable for the direct process. However, for both  $^3\text{He}$  and  $^4\text{He}$  we find that the data scales with  $T^4/\omega$  (Fig. 13). This well-defined scaling indicates that there exists one dominant process for the enhancement of the TLS relaxa-

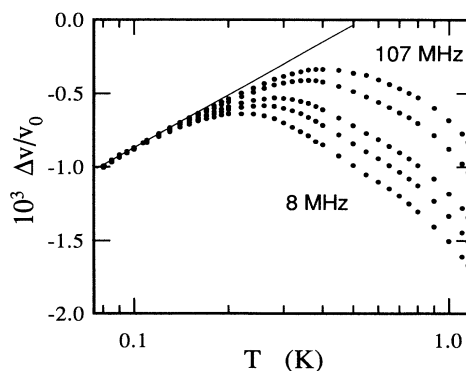


FIG. 12. The sound speed in Vycor with the pores filled with  $^4\text{He}$ . Data are shown for 8, 15, 24, 64, and 107 MHz. The straight line indicates the resonant contribution.

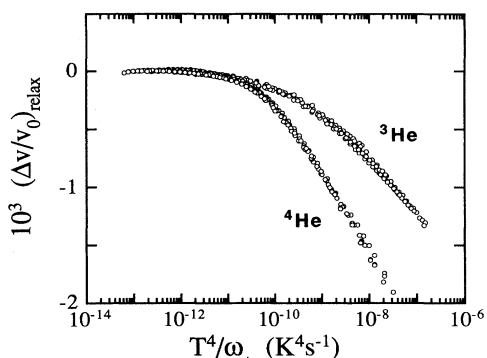


FIG. 13. The relaxation contribution to the sound speed in Vycor with the pores filled with either  $^3\text{He}$  or  $^4\text{He}$ , plotted vs  $T^4/\omega$ . The data are for the following frequencies:  $^4\text{He}$ : 5, 8, 15, 24, 64, and 107 MHz;  $^3\text{He}$ : 5, 8, 16, 32, and 98 MHz.

tion rates. Both  $^3\text{He}$  and  $^4\text{He}$  support this process, although its strength is greatly reduced with  $^3\text{He}$ .

The attenuation data give a more complicated picture (Fig. 14). The results for  $^4\text{He}$  resemble what we would expect on the basis of sound velocity measurements. Over a reasonably wide temperature range (below 1.2 K) we observe again a scaling with  $T^4/\omega$ . In the same temperature range over which the relaxation contribution to the sound speed becomes important, the attenuation rises to its plateau value. However, at low temperatures we do not see a return of the attenuation to the empty Vycor background value. Apparently there is a second attenuation mechanism, not associated with the  $T^4/\omega$  process. This becomes even more apparent with  $^3\text{He}$ . From the corresponding sound velocity measurements one would expect a very modest contribution to the attenuation, and indeed, the change in attenuation is small, but over all the attenuation remains high, even down to 100 mK.

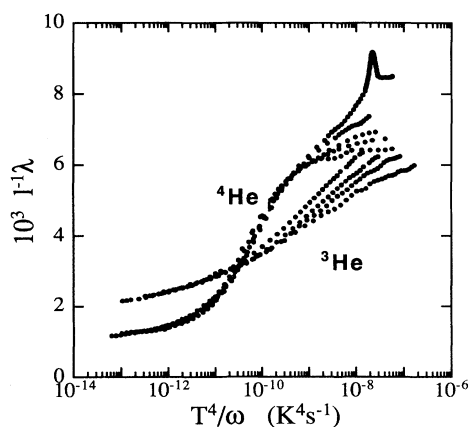


FIG. 14. The attenuation corresponding to Fig. 13. The curves appear from top to bottom in descending order of frequency. The peak in the 107-MHz data for  $^4\text{He}$  is associated with the superfluid transition.

## DISCUSSION

The change in the acoustic properties on adsorption of thin helium film may be understood in the following way. The Vycor surface creates a random potential for the helium atoms with low-lying localized states. At low coverage the helium atoms will gradually fill these states. Strongly bound, they cannot interact effectively with the TLS. Additional helium will occupy states that are increasingly more easily excited and are available for helium-TLS interactions and with both  $^3\text{He}$  and  $^4\text{He}$  we see a gradual increase in the relaxation rates. At some point these states are filled and atoms will start to condense in extended states. At this stage we may expect a significant difference between  $^3\text{He}$  and  $^4\text{He}$  because now their difference in statistics becomes important. In the case of  $^4\text{He}$  the film becomes superfluid below some temperature. This appears to have a strong effect, especially on the low-temperature attenuation. If we attribute the low-temperature attenuation to an interaction between the dense surface layer and the TLS, the conclusion must be that the superfluid transition is accompanied by a significant change in the structure of this layer. The TLS relaxation rates drop, indicating that there are few excitations available for the TLS to interact with. Specific-heat measurements support this assertion. Chan *et al.*<sup>16</sup> show that the heat capacity of films just below the critical coverage is larger than that of thin superfluid films at the same temperature. It appears that the entropy of the dense layer drops significantly when the film becomes superfluid. It is clearly incorrect to treat the dense layer as an inert substrate on top of which forms an independent superfluid film.<sup>17</sup> With  $^3\text{He}$  there is of course no transition in this temperature range and no change in the influence of the dense layer is observed.

The most puzzling aspect of our experiment is the apparent discrepancy between the results of the sound speed and the attenuation measurements in the case where the pores are completely filled. Because the viscous penetration depth in helium at our ultrasonic frequencies exceeds the pore size, the liquid moves with the glass matrix and viscous losses are expected to be small. It should also be noted that since we use a shear mode there is no volume change, at least not at length scales comparable to the ultrasonic wavelength, and so there is no attenuation associated with the compression and expansion of the liquid. Therefore, our expectation was that, apart from the effect of changes in the effective total density of the sample on the sound speed, all changes in the acoustic properties would be attributable to TLS effects. An increased attenuation should be accompanied by a changing sound speed. Around 100 mK this does not seem to be the case, and it appears that there is another attenuation mechanism, not directly related to interactions with the TLS. However, at higher temperatures the attenuation approaches the same TLS plateau value as in empty Vycor.

A further complication is that both helium isotopes show the  $T^4/\omega$  process, although at these temperatures the liquids are dominated by quite different classes of excitations. Both liquids support longitudinal phonons. The problem is that below 1 K the wavelength of the dominant thermal phonons exceeds the pore size. At



long wavelengths the phonons are modes of the combined helium-Vycor system and essentially completely determined by the acoustic properties of the Vycor. However, superfluid helium supports a second class of modes in the form of fourth sound. Thermally excited fourth sound modes are free to propagate through the helium. In view of their low sound speed the density of states is expected to be high in which case they can have a considerable effect on the TLS relaxation rates, provided there is a suitable coupling mechanism. However, in normal  $^3\text{He}$  fourth sound is absent.

In conclusion, we have studied the low-temperature acoustic properties of Vycor and find that these are strongly influenced by the adsorption of helium in the pore space. To some extent this can be explained by interactions between excitations in the helium and the TLS, analogous to the normal phonon-TLS interactions in regular glasses. With the pores completely filled, we find a considerable increase in the attenuation at low temperatures which is not accompanied by a corresponding

change in sound speed, and this simple picture breaks down. At the same time we find a scaling for the relaxation contribution to the sound speed with  $T^4/\omega$ . This seems to indicate that at higher temperatures there is a single dominant interaction mechanism between the helium and the TLS, for both  $^3\text{He}$  and  $^4\text{He}$ . Furthermore, we find that with  $^4\text{He}$  in the pores the attenuation at low temperature drops when a coverage close to  $n_c$  is exceeded. This seems to rule out the inert layer model for the adsorption of  $^4\text{He}$ .

#### ACKNOWLEDGMENTS

Acknowledgment is made to the Donors of The Petroleum Research Fund, administered by the American Chemical Society, for the partial support of this research. This work was also supported by a grant from the Natural Sciences and Engineering Research Council of Canada.

\*Present address: Department of Physics, University of Exeter, Exeter EX4 4QL, U.K.

<sup>1</sup>General reviews include: *Amorphous Solids, Low Temperature Properties*, edited by W. A. Phillips (Springer, Berlin, 1981); S. Hunklinger and A. K. Raychaudhuri, *Prog. Low Temp. Phys.* **9**, 265 (1986); W. A. Phillips, *Rep. Prog. Phys.* **50**, 1657 (1987).

<sup>2</sup>W. A. Phillips, *J. Low Temp. Phys.* **7**, 351 (1972).

<sup>3</sup>P. W. Anderson, B. I. Halperin, and C. M. Varma, *Philos. Mag.* **25**, 1 (1972).

<sup>4</sup>H. Schubert, P. Leiderer, and H. Kinder, *Phys. Rev. B* **26**, 2317 (1982).

<sup>5</sup>J. R. Beamish, A. Hikata, and C. Elbaum, *Phys. Rev. Lett.* **52**, 1790 (1984).

<sup>6</sup>M. H. W. Chan *et al.*, *Bull. Am. Phys. Soc.* **33**, 443 (1988); and (private communication).

<sup>7</sup>P. Wiltzius, F. S. Bates, S. B. Dierker, and G. D. Wignall, *Phys. Rev. A* **36**, 2991 (1987).

<sup>8</sup>P. Levitz, G. Ehret, S. K. Sinha, and J. M. Drake, *J. Chem. Phys.* **95**, 6151 (1991).

<sup>9</sup>For a more detailed discussion of the ultrasonic system, see N. Mulders and J. R. Beamish, in *Quantum Fluids and Solids-1989*, edited by G. G. Ihas and Y. Takano (AIP, New York,

1989), p. 399.

<sup>10</sup>P. Doussineau, C. Frenois, R. G. Leisure, A. Levelut, and J.-Y. Prieur, *J. Phys. (Paris)* **41**, 1193 (1980).

<sup>11</sup>A. J. Leggett, *Physica B* **169**, 322 (1991); S. N. Coppersmith, *Phys. Rev. Lett.* **67**, 2315 (1991); C. C. Yu, *ibid.* **63**, 1160 (1989); M. I. Klinger, *Usp. Fiz. Nauk.* **152**, 623 (1987) [*Sov. Phys. Usp.* **30**, 699 (1988)].

<sup>12</sup>K. Kassner and R. Silbey, *J. Phys. C* **1**, 4599 (1989).

<sup>13</sup>J. F. Berret and M. Meissner, *Z. Phys. B* **70**, 65 (1988).

<sup>14</sup>D. McQueeney, G. Agnolet, and J. D. Reppy, *Phys. Rev. Lett.* **52**, 1325 (1984).

<sup>15</sup>D. Finotello, K. A. Gillis, A. Wong, and M. H. W. Chan, *Phys. Rev. Lett.* **61**, 1954 (1988).

<sup>16</sup>M. H. W. Chan, D. Finotello, K. A. Gillis, S. Mukherjee, and A. P. Y. Wong, in *Excitations in Two-dimensional and Three-dimensional Quantum Fluids*, edited by A. F. G. Wyatt and H. J. Lauter (Plenum, New York, 1991), p. 301.

<sup>17</sup>For a discussion of the possibility of the existence of an inert layer and its relation to the superfluid onset transition, see M. P. A. Fisher, P. B. Weichmann, G. Grinstein, and D. S. Fisher, *Phys. Rev. B* **40**, 546 (1989); D. K. K. Lee and J. M. F. Gunn, *J. Low Temp. Phys.* **89**, 101 (1992).